Carrier compensation near tail region in aluminum- or boron-implanted 4H–SiC (0001)

Y. Negoro,[a] T. Kimoto, and H. Matsunami
Department of Electronic Science and Engineering, Kyoto University, Kyotodaigaku-katsura, Nishikyo, Kyoto 615-8510, Japan

(Received 28 July 2004; accepted 13 July 2005; published online 25 August 2005)

Electrical behavior of implanted Al and B near implant-tail region in 4H–SiC (0001) after high-temperature annealing has been investigated. Depth profiles of Al and B acceptors determined by capacitance-voltage characteristics are compared with those of Al and B atoms measured by secondary-ion-mass spectrometry. For Al^+ (aluminum-ion) implantation, slight in-diffusion of Al implants occurred in the initial stage of annealing at 1700 °C. The profile of the Al-acceptor concentration in a "box-profile" region as well as an "implant-tail" region is in good agreement with that of the Al-atom concentration, indicating that nearly all of the implanted Al atoms, including the in-diffused Al atoms, work as Al acceptors. Several electrically deep centers were formed by Al^+ implantation. For B^+ (boron-ion) implantation, significant out- and in-diffusion of B implants occurred in the initial stage of annealing at 1700 °C. A high density of B-related *D* centers exists near the tail region. In the tail region, the sum of B-acceptor concentration and *D*-center concentration corresponds to the B-atom concentration. C^+ (carbon-ion) coimplantation with a ten times higher dose than B^+ effectively suppressed the B diffusion, but additional deep centers were introduced by C^+ coimplantation. © *2005 American Institute of Physics*. [DOI: 10.1063/1.2030411]

I. INTRODUCTION

Silicon carbide (SiC) is an attractive semiconductor material for high-power electronic devices.[1] The device processing of SiC is one of the crucial issues for realizing high-performance devices. For example, SiC cannot be doped effectively by thermal diffusion because of the low diffusion coefficients of dopants.[2] Consequently, there is currently considerable interest in using ion implantation for doping SiC. For SiC device processes, selective *n*-/*p*-type doping with precisely designed donor/acceptor concentrations is a fundamental requirement. Typical applications include n^+-type doping ($\geqslant 10^{20}$ cm^{-3}) for source/drain in field-effect transistors (FETs), *n*-type doping (10^{16}–10^{18} cm^{-3}) for reduced surface field (RESURF) regions in lateral metal-oxide-semiconductor FETs (MOSFETs), p^+-type doping ($\geqslant 10^{20}$ cm^{-3}) for the anode of *p*-*i*-*n* diodes, and *p*-type doping (10^{17}–10^{18} cm^{-3}) for *p* wells in FETs and junction termination extension (JTE) structures to alleviate electric field crowding in devices.

In the case of *n*-type doping, nitrogen-ion (N^+) and phosphorus-ion (P^+) are commonly employed. For n^+-type doping, P^+ implantation has attracted increasing attention[3] and resulted in a very low sheet resistance of about 50 Ω/□.[4,5] A detailed comparison of N^+ and P^+ implantations for *n* type (10^{17}–10^{18} cm^{-3}) has also been conducted.[6]

On the other hand, implantation of aluminum-ion (Al^+) and boron-ion (B^+) is used for *p*-type doping. Al^+ implantation is particularly attractive for forming heavily doped p^+ regions with reasonable sheet resistances, because Al acceptors have a smaller ionization energy [190 meV (Ref. 7)] than B acceptors [285 meV (Ref. 8)] in 4H–SiC. A minimum sheet resistance of 2.3 kΩ/□ has been achieved by Al^+ implantation with a very high dose of 3.0×10^{16} cm^{-2} and high-temperature annealing at 1800 °C for a short time of 1 min.[9] B^+ implantation is effective in forming deep *p*-*n* junctions, because B atoms reach larger projected ranges due to their lighter mass.

To form moderately doped *p*-type (10^{17}–10^{18} cm^{-3}) regions, both Al^+ and B^+ implantations have been employed.[10,11] So far, it has been reported that Al and B implants in 4H–SiC are electrically activated by postimplantation annealing at around 1600 and 1700 °C, respectively.[10] In the case of B^+ implantation, this temperature treatment, however, causes rapid diffusion of B atoms toward the surface and thus a strong decrease of the total B concentration in the samples.[12,13] In addition, a pronounced in-diffusion of B is observed.[12–14] It has been suggested that B atoms diffuse by a kick-out mechanism, and nonequilibrium concentrations of native point defects introduced during the implantation.[15] It is important to suppress the out-/in-diffusion during high-temperature annealing as well as to raise the electrical activation of implanted B atoms.

In order to create the *p*-type regions suitable for devices, much attention must be paid to the electrical behavior of implants near a "tail" region, in addition to the electrical activation of implants. Although significant in- and out-diffusion of implanted B atoms during high-temperature annealing have been reported, an investigation on electrical behavior of in-diffused B atoms near the tail region has not been conducted. It is yet unknown whether the in-diffused B atoms work as shallow acceptors or form electrically deep centers. For Al^+ implantation, detailed investigation on electrical properties of the tail region has also been missing. Although the electrical activation and deep centers near the

[a]Electronic mail: negoro@semicon.kuee.kyoto-u.ac.jp

TABLE I. Implant energy and dose ratio for Al^+ and B^+ implantations.

Al		B	
Energy (keV)	Dose ratio	Energy (keV)	Dose ratio
120	0.48	70	0.41
90	0.17	50	0.14
60	0.17	40	0.13
30	0.12	30	0.12
10	0.06	20	0.12
		10	0.08

tail region strongly influence the characteristics of *p-n* junctions such as *p* wells in FETs, it is difficult to analyze the electrical properties near the tail region by Hall-effect measurements.

In this study, we have investigated the electrical behavior of acceptor-type implants (Al^+ and B^+) near the implant-tail region in 4H–SiC (0001) after high-temperature annealing. Depth profiles of Al and B acceptors determined by *C-V* measurements are compared with those of Al and B atoms. Electrically deep centers and their depth profiles are examined by using capacitance transient measurements.

II. EXPERIMENTS

The starting material was Al-doped *p*-type epitaxial layers ($N_a - N_d$: 6.0×10^{15} cm^{-3}; thickness: 10 μm) on 8° off-axis *p*-type 4H–SiC (0001) substrates purchased from Cree. The thickness and resistivity of the substrates are 330 μm and 3.6 Ω cm, respectively. Multiple implantation of Al^+ or B^+ was carried out at room temperature (RT) to form a 0.2 -μm-deep box profile of Al or B. Since the reduction of implantation temperature is of great importance from the viewpoint of productivity, implantations were employed at RT. It should be noted that some of the samples were implanted with B^+ at an elevated temperature of 500 °C for comparison. The implantation energies and the corresponding ratio of the doses for each dopant are summarized in Table I. The total dose was 2×10^{13} cm^{-2}, which corresponds to a concentration of 1×10^{18} cm^{-3}. For a part of the B^+-implanted samples, carbon-ion (C^+) implantation was employed prior to B^+ implantation. The C^+ dose was 100%, 200%, or 1000% of implanted B^+ dose. The coimplantation of C^+ is expected to suppress the out- and in-diffusion of B atoms during high-temperature annealing,[14,16] because excess C interstitials effectively raise the probability for B atoms to occupy Si sublattice sites where they act as shallow acceptors.[8]

After forming a graphite cap on the whole surface of the implanted samples to suppress surface roughening,[17] postimplantation annealing was performed in an Ar ambient at 1700 °C for 1 min or 30 min using a chemical-vapor deposition (CVD) reactor. The graphite cap was removed in an O_2 ambient at 900 °C for 30 min;[17] by this process very little oxidation of the SiC surface takes place. Ti Schottky contacts (thickness: 100 nm; diameter: 0.3–1.0 mm) were thermally deposited on the implanted samples for capacitance-voltage (*C-V*) and capacitance transient measurements. The backside Ohmic contacts to the p^+ substrates were Ti/Al (10 nm/200 nm) annealed at 950 °C for 1 min. This annealing step was employed prior to the Schottky-contact formation.

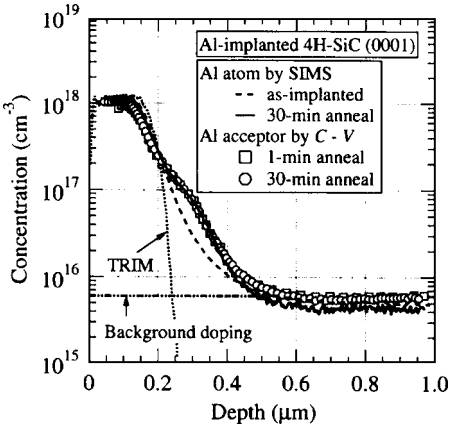

FIG. 1. Depth profiles of Al-atom concentration obtained from SIMS and Al-acceptor concentration from *C-V* analyses after annealing at 1700 °C.

Depth profiles of Al- or B-acceptor concentration were obtained by analyzing *C-V* characteristics of Ti/implanted *p* -SiC Schottky structure. *C-V* measurements were conducted with a probe frequency of 1 MHz at various temperatures (RT-600 K). In the case of metal/*p*-type semiconductor Schottky structure, the depleted region in the semiconductor is extended when a positive voltage is applied to the metal. Electrically deep defect centers were investigated by deep-level transient spectroscopy (DLTS) with a transient length of 0.2 s and isothermal capacitance transient spectroscopy[18] (ICTS) using DL8000 from Accent Optical Technologies. For the analysis of DLTS spectra, a Fourier-transform analysis[19] of the measured transients was employed, together with an Arrhenius-plot analysis for the determination of capture cross section, energy level, and trap concentration. The temperature-independent capture cross section was assumed when analyzing the DLTS and ICTS data.

III. RESULTS AND DISCUSSION

A. Electrical characterization of aluminum-implanted 4H–SiC

Figure 1 shows the depth profiles of Al-atom concentration obtained from secondary-ion-mass spectrometry (SIMS) and net Al-acceptor concentration obtained from *C-V* at RT after annealing at 1700 °C for 1 and 30 min. Note that, in the region deeper than 0.5 μm, the Al concentration was measured to be 6.0×10^{15} cm^{-3} both from SIMS and *C-V*, which is consistent with the Al concentration of the epilayer. The implant tail (about 0.3 μm deep) of the SIMS profile slightly shifts by approximately 50 nm toward the deeper side by annealing at 1700 °C regardless of the annealing time, compared to the as-implanted profile. This result indicates that in-diffusion of Al atoms occurred in the initial stage (<1 min) of annealing at 1700 °C. From the *C-V* analysis, it is found that the profiles of acceptor concentration for 1-min- and 30-min-annealed samples are almost the same and in good agreement with the SIMS profile. Nearly

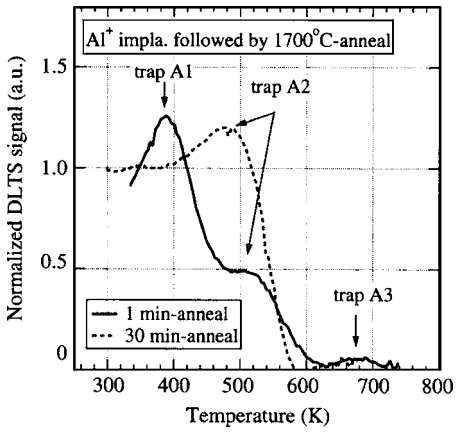

FIG. 2. DLTS signals from the samples implanted with Al^+ and annealed at 1700 °C.

all of the implanted Al atoms, including the in-diffused Al atoms, behave as Al acceptors (~100% electrical activation).

It should be noted that the electrical activation ratio here obtained from the *C-V* analysis is defined as the ratio of the acceptor (electrically active impurity) concentration to the implanted impurity concentration. In several investigations on Hall-effect measurements, the electrical activation is defined as the ratio of free hole concentration at RT to the implanted impurity concentration, and in some cases the ratio of acceptor concentration (obtained by fitting Hall data) to the implanted impurity concentration. Bluet *et al.* defined the activation ratio by using the free hole concentration at RT.[20] In this case, the electrical activation ratio in high-dose Al^+-implanted 4H–SiC may not be 100% because of the large ionization energy of Al acceptors.[11,20] Saks *et al.* made the curve fitting of temperature-dependent Hall data and estimated the actiavation ratio (acceptor concentration/Al concentration) to be close to 100%,[11] which is in agreement with the present results. For more intensive studies on the electrical behavior of Al^+ implants, Hall measurements should be employed and compared with the results obtained from the *C-V* analysis. Another important issue to be focused on is whether implanted Al atoms occupy a Si sublattice site or a C sublattice site. Although we have not paid much attention to this issue, Jones *et al.* reported that they did not detect an Al_{Si} electron-paramagnetic-resonance (EPR) signal in Al-implanted 4H–SiC, but they did in epitaxially grown material with the same Al concentration.[21]

DLTS and ICTS measurements revealed that there exist several deep centers with different activation energies within the lower half of the band gap. Figure 2 shows the normalized DLTS signals obtained in the 1-min- and 30-min-annealed samples. The reverse bias was kept at +10 V and pulsed to 0 V with a pulse duration of 1.0 s. In this study, pulse durations of 100 ms and 1.0 s were employed, but no significant difference was observed. The transient length used in these measurements was 0.2 s. Note that the depletion depth at a reverse bias of +10 V was about 0.12 μm. For the 1-min-annealed sample (solid curve), three peaks (denoted as traps A1, A2, and A3) are found at about 380, 500, and 700 K, respectively. The parameters of these three traps obtained by the Arrhenius-plot analysis are summarized in Table II. The highest peak in the DLTS signal for the 1-min-annealed sample is trap A1 with an activation energy of 0.82 ± 0.03 eV and a concentration of 5×10^{15} cm^{-3}. For the 30-min-annealed sample, however, the highest peak is related not to trap A1 but to trap A2 with an activation energy of 1.01 ± 0.05 eV and a concentration of 5×10^{15} cm^{-3}. It may be possible that traps A1 and A2 are associated with one defect that has changed from one configuration to another after a longer annealing time. Trap A3 with an activation energy of 1.70 ± 0.10 eV is a midgap level which might be identical to the P1 center observed in *p*-type 4H–SiC.[22] Although several deep centers were formed by Al^+ implantation, the concentrations of these traps are about three orders of magnitude lower than the implanted Al concentration. Consequently, the change in trap concentration by the prolonged annealing time is not reflected in the (Al) acceptor concentration determined by *C-V* measurements. These results also indicate that the high electrical activation of Al acceptors could be achieved in these samples. Note that since the DLTS measurements were carried out in the temperature range from RT to 750 K in the present case, a deep center with a relatively low activation energy such as HS1 center[23] (activation energy: 0.35 eV) could not be detected. There may exist the HS1 center in the Al^+-implanted samples. The concentration of the HS1 center, however, may be much lower than the Al-acceptor concentration in the present samples, taking into account that the experimental results in Fig. 1 show almost perfect electrical activation.

TABLE II. Parameters of deep centers obtained from the DLTS data of 4H–SiC implanted with Al^+ and annealed at 1700 °C for 1 min.

Trap	A1	A2	A3
Activation energy E_a (eV)	0.82 ± 0.03	1.01 ± 0.05	1.70 ± 0.1
Capture cross section σ (cm^2)	1×10^{-15}	2×10^{-16}	4×10^{-14}
Trap concentration N_t (cm^{-3})	5.2×10^{15}	2.3×10^{15}	3.2×10^{14}

From the investigation of the Al^+-implanted samples shown above, the following features were obtained: Slight in-diffusion of Al implants occurred in the initial stage of annealing at 1700 °C. The in-diffused Al implants near the tail region worked as Al acceptors. Nearly all of the implanted Al atoms, including the in-diffused Al atoms, were activated by annealing at 1700 °C even for 1 min. Several deep centers were formed by Al^+ implantation. The energy levels of the centers were obtained to be 0.82 ± 0.03, 1.01 ± 0.05, and 1.70 ± 0.1 eV above the valence band. The concentrations of the centers were about three orders of magnitude lower than that of the implanted Al-atom concentration.

B. Electrical characterization of boron-implanted 4H–SiC

Figure 3 shows the depth profiles of the B-atom concentration (SIMS) and "apparent" B-acceptor concentration (*C-V* at RT) after annealing at 1700 °C for 1 and 30 min. Here, the apparent B-acceptor concentration was obtained by subtracting the Al-acceptor concentration (background doping of 6.0×10^{15} cm^{-3}) from the net acceptor concentration (*C-V*

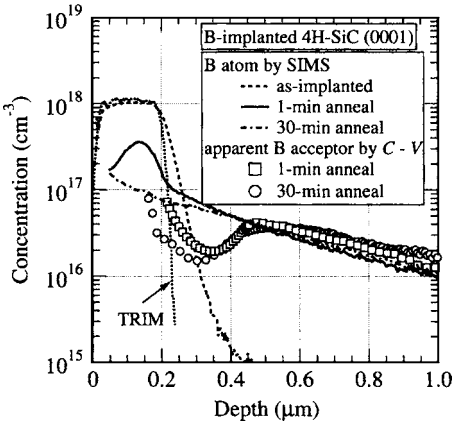

FIG. 3. Depth profiles of B-atom concentration obtained from SIMS and B-acceptor concentration from *C-V* analyses after annealing at 1700 °C.

analysis). SIMS measurements revealed that both out- and in-diffusion of B atoms are strongly pronounced by annealing at 1700 °C even for a short time of 1 min. The apparent B-acceptor profiles at RT relatively agree with the SIMS profiles in the depth range of 0.5–1.0 μm. However, the acceptor profile shows a depression near the implant tail (0.2–0.4 μm), where a high density of defects introduced by implantation may exist and compensate B acceptors.

In order to investigate electrically deep centers in the B^+-implanted samples, ICTS measurements were conducted. ICTS is an effective method to characterize deep levels, concentration of which reaches the same order as the doping concentration.[24] Figure 4(a) shows the ICTS spectra of the B^+-implanted sample at 230–320 K. The reverse bias was kept at +5 V and pulsed to 0 V with a pulse duration of 100 ms. The Arrhenius plot of the time constant of hole emission from the deep centers is shown in Fig. 4(b). The ICTS measurements revealed one major deep center with an activation energy of 0.47 eV, so-called *D* center,[25] which may be related to B atoms. The capture cross section of the *D* center was 3×10^{-15} cm^2. The depth analysis of the *D* center was carried out by changing the reverse bias from 0 to +30 V in the ICTS measurements with keeping a pulse height of 2, 5, or 10 V. The result is plotted by the open circles with the error bars in Fig. 5(a). The depth analysis revealed that a higher density of the deep center exists in the depth range of 0.2–0.4 μm, where the deep center concentration reaches the same order as the B-acceptor concentration. This result indicates that the *D* center is responsible for the depression in the depth profile of B-acceptor concentration at RT shown in Fig. 3.

With increasing temperature of the *C-V* measurements, the depression in B-acceptor concentration becomes smaller as in Figs. 5(a) and 5(b). At 450 K, no depression is found near the tail. These results are attributed to the following causes: Holes captured by the deep centers (*D* center) cannot respond to the signal of the *C-V* measurement (probe frequency of 1 MHz) at RT, because the probe frequency is much higher than the inverse of time constant for hole emission from the deep centers. If the deep centers are positively charged due to the hole capture (donorlike hole trap), the net acceptor concentration should be reduced, resulting in the

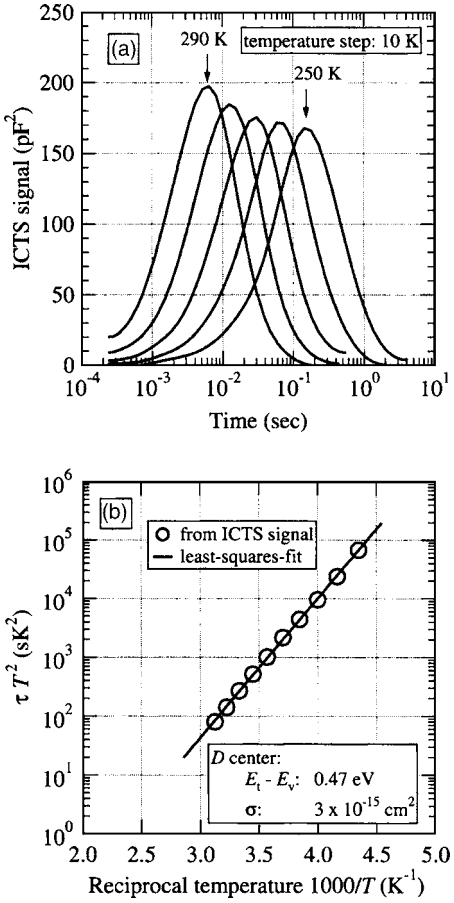

FIG. 4. ICTS data of the samples implanted with B^+ and annealed at 1700 °C: (a) ICTS signals and (b) Arrhenius plot of time constant for hole emission from the deep centers.

depression. As increasing the measurement temperature, the time constant of hole emission becomes shorter, which enables the deep centers to respond to the measurement signal. The other possible explanation for the depression is that the deep centers (*D* centers) are neutral due to the hole capture (deep acceptor) at RT. If so, the apparent B-acceptor concentration at 450 K or higher should be the sum of the shallow B acceptors and the deep B acceptors (the deep centers). Assuming that the deep center is a deep acceptor (the latter case), the fairly good agreement between the B-atom profile and the apparent B-acceptor profile measured at 450 K (shown in Fig. 5) is reasonably explained. If the *D* centers are assumed to be donorlike (the former case), the B-acceptor concentration at 450 K should be lower than the B-atom profile by the concentration of the *D* center, which does not agree with the experimental results shown in Fig. 5. It is not known whether the *D* center and the deep B center observed by optical experiments[26] are the same, and if so, whether these centers are donors or acceptors. Troffer *et al.* reported that the *D* center acts as a donor (donorlike hole trap) from analyses of double correlated DLTS.[25] The results obtained in this study contradict the double correlated DLTS data,[25] but support the data based on optical experiments.[26]

From the investigation of the B^+-implanted samples shown above, the following features were obtained: Significant out- and in-diffusion of B implants occurred in the ini-

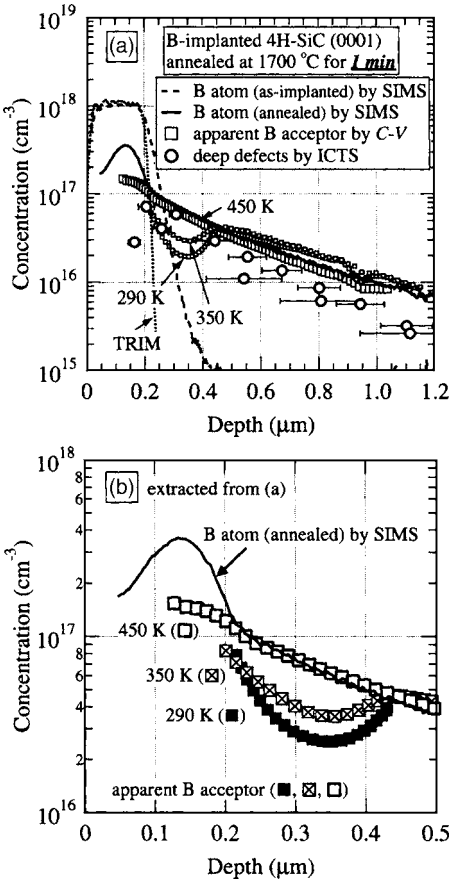

FIG. 5. (a) Depth profiles of concentrations for B atoms (SIMS) and deep centers (ICTS) at RT, and concentration for B acceptors (*C-V*) measured at various temperatures. Note that the B-acceptor concentrations at 290, 350, and 450 K are plotted by the same symbol of open squares; (b) depth profiles of B atoms and B acceptors in the depth range of 0–0.5 μm extracted from (a).

tial stage of annealing at 1700 °C. Most of the in-diffused B implants worked as B acceptors. A high density of B-related *D* center exists near the tail region, which brings a depression in the depth profile of B-acceptor concentration at RT. It should be noted that a depth profile of B acceptors in the samples implanted at 500 °C was not significantly different from that in the samples implanted at RT. However, the concentration of the *D* center was reduced by a factor of 1.5–2.0 compared to RT-implanted samples. Since we used the *C-V* measurements to analyze electrical activation of implants near the implant-tail region, we were not able to obtain other parameters such as free hole concentration and mobility. To characterize such properties, a differential Hall-effect measurement may be an effective technique.

C. Electrical characterization of B^+-/C^+-coimplanted 4H–SiC

In the previous part, the electrical behavior of implanted B atoms near the tail region was discussed. From the device process and device-design points of view, suppression of the in- and out-diffusion of B atoms and the control of the B-acceptor profile are strongly required. B^+ and C^+ coimplantations have been proposed to suppress the diffusion of B atoms.[14,16] However, a depth profile of the B-acceptor concentration in B^+-/C^+-coimplanted samples is still unknown. Deep centers introduced by additional C^+ coimplantation must also be investigated. Here, annealing time was fixed at 1 min for C^+ coimplantation experiments because of the following two reasons. One reason is that no significant difference in electrical activation of B^+ implants is observed between the 1-min-annealed and 30-min-annealed samples for single B^+ implantation as far as annealing was done at 1700 °C (not shown). The other reason is that even by 1 -min annealing, diffusion of implanted B atoms is significant in the case of single B^+ implantation, as shown in Fig. 3.

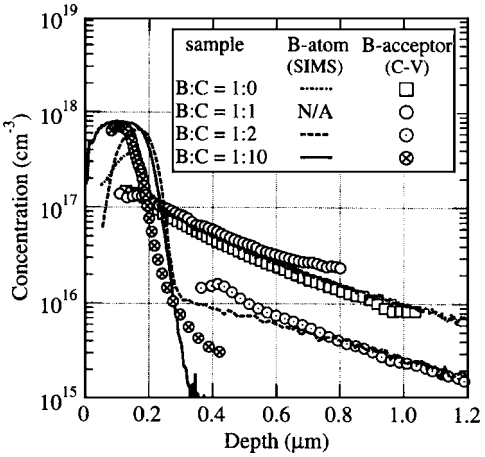

FIG. 6. Depth profiles of B-atom concentration and B-acceptor concentration at 600 K in B^+-/C^+-coimplanted 4H–SiC. The ratio of B:C for each sample is indicated in the figure.

Figure 6 shows the depth profiles of the B-atom concentration (SIMS) and B-acceptor concentration (*C-V* at 600 K) for the C^+-coimplanted samples after annealing at 1700 °C for 1 min. As is the case with the only B^+-implanted sample, significant in-diffusion was observed in the C^+-coimplanted samples with the B:C ratios of 1:1 and 1:2. It seems that the C^+ doses for the two samples are not high enough to suppress the diffusion. Note that the B-acceptor concentration shows good agreement with the B-atom profile in the deep in-diffused tail for these samples. On the other hand, high-dose C^+ coimplantation with B:C of 1:10 remarkably suppressed the diffusion. This is in good agreement with the report by Kumar *et al.*[16] Although the B acceptor-concentration profile at 600 K is almost the same as that of the B-atom concentration in the sample with B:C=1:10, a profile of B-acceptor concentration at RT was quite different from those at high temperatures above 550 K (not shown). This implies that the *D* center and/or other deep centers might compensate B acceptors.

It is of great importance to investigate deep centers introduced by additional C^+ coimplantation. Figure 7 shows the DLTS spectra of (a) B^+-implanted, (b) B^+-/C^+-coimplanted (B:C=1:2), and (c) B^+-/C^+-coimplanted (B:C=1:10) samples. The reverse bias was kept at +10 V and pulsed to 0 V with a pulse duration of 1.0 s. The transient length used here was 0.2 s. The peak at about 250 K related to the *D* center becomes less dominant by increasing the dose of coimplanted C^+. This result indicates that the formation of the *D* center was suppressed by excess C^+

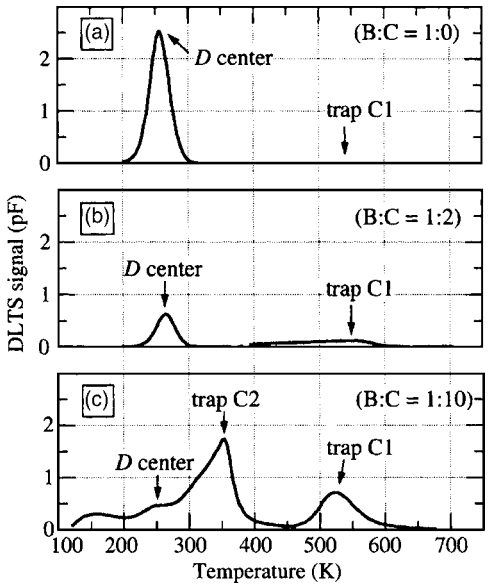

FIG. 7. DLTS spectra for B^+-/C^+-coimplanted 4H–SiC: (a) only B^+ implanted, (b) B^+/C^+ coimplanted (B:C=1:2), and (c) B^+/C^+ coimplanted (B:C=1:10).

coimplantation in agreement with previous work.[16,27] However, the *D* center still exists even in the B^+-/C^+-coimplanted (B:C=1:10) sample, as shown in Fig. 7(c).

In addition to the *D* center, DLTS peaks due to other deep centers were observed at higher temperatures in the B^+-/C^+-coimplanted samples. Here, the peaks at 550 and 400 K are named as traps C1 and C2, respectively. Since the concentrations of those traps are relatively high, ICTS was employed to characterize the trap parameters accurately. From the Arrhenius plots of the ICTS data shown in Fig. 8, the activation energy and the capture cross section for trap C1 were estimated to be 1.55 ± 0.10 eV and 1×10^{-12} cm^2, respectively. The concentration of trap C1 increases with increasing the dose of C^+, resulting in the concentration of 3.5×10^{16} cm^{-3} in the sample with B:C of 1:10. It should be noted that trap C1 exists even in the only B^+-implanted sample with a much lower concentration of $\sim10^{14}$ cm^{-3}. In the case of the B^+-/C^+-coimplanted (B:C=1:10) sample, trap C2 is the most dominant trap in the DLTS spectrum [see Fig. 7(c)]. The activation energy and the capture cross section for trap C2 were estimated to be 0.69 ± 0.05 eV and 8×10^{-16} cm^2. The concentration of trap C2 was about 2×10^{17} cm^{-3}, almost the same order as that of B acceptor. These results indicate that C^+ coimplantation brings additional deep centers and these centers compensate B acceptors. Recent theoretical calculation by Gali *et al.*[28] has predicted that a very stable complex of "$B_{Si}+(C_i)_2$" (B_{Si}: B occupying a Si sublattice site; C_i: C interstitial) will form when B^+ ions are coimplanted with an excess dose of C^+. The binding energy of the complex $B_{Si}+(C_i)_2$ is calculated to be 4.4 eV, resulting in a thermally very stable complex. The complex has negative-*U* behavior and is located at around $E_V+0.9$ eV, where E_V is the energy at the top of the valence band. The complex of $B_{Si}+(C_i)_2$ is probably the same as trap C2 presented in this study.

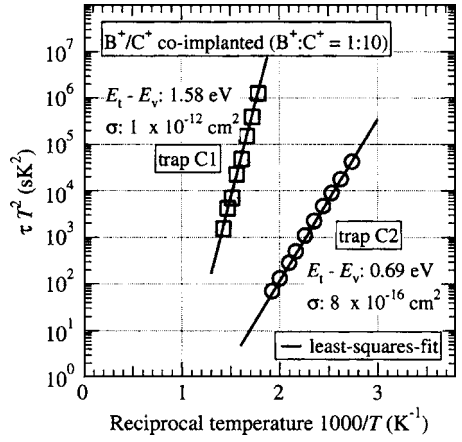

FIG. 8. Arrhenius plot of the ICTS data obtained from the B^+-/C^+-coimplanted (B:C=1:10) sample.

From the investigation of the B^+-/C^+-coimplanted samples shown above, the following features were obtained: Even when C^+ ions were coimplanted with a dose twice that of B^+, significant out- and in-diffusion of B implants occurred during annealing at 1700 °C for 1 min. Very high-dose C^+ coimplantation (B:C=1:10) finally suppressed the out- and in-diffusion during the annealing, but high concentrations of additional deep centers were introduced in the B^+-/C^+-coimplanted sample. These centers compensate most of B acceptors at RT.

IV. CONCLUSION

We investigated the electrical behavior of implanted Al and B atoms near the tail region in 4H–SiC (0001) after high-temperature annealing. For Al^+ implantation, slight in-diffusion of Al implants occurred in the initial stage of annealing at 1700 °C. Nearly all of the implanted Al atoms, including the in-diffused Al atoms, were activated by annealing at 1700 °C even for 1 min and worked as Al acceptors. Several electrically deep centers were formed by Al^+ implantation. The concentrations of the centers were three to four orders of magnitude lower than that of the implanted Al-atom concentration. For B^+ implantation, significant out- and in-diffusion of B implants occurred in the initial stage of annealing at 1700 °C. Most of the in-diffused B implants worked as B acceptors. A high density of B-related *D* center exists near the "tail" region, which brings a depression in the depth profile of B-acceptor concentration (compensation) at RT. To suppress the B diffusion, a ten times higher dose of C^+ coimplantation was effective. However, high concentrations of additional deep centers were introduced by such high-dose C^+ coimplantation.

ACKNOWLEDGMENTS

This work was supported by Grant-in-Aid for JSPS fellows [for one of the authors (Y.N.)], Grant-in-Aid for Fundamental Research (No. 16360153), and Grant-in-Aid for the 21st Century COE program 14213201, from the Ministry of Education, Culture, Sports, Science and Technology of Japan, and also by TEPCO Research Foundation [for one of the authors (T.K.)].

[1]H. Matsunami and T. Kimoto, Mater. Sci. Eng., R. **20**, 125 (1997).
[2]Yu. A. Vodakov and E. N. Mokhov, *Silicon Carbide* 1973 (University of South Carolina Press, Columbia, SC, 1974), p. 508.
[3]M. Laube, F. Schmid, G. Pensl, G. Wagner, M. Linnarsson, and M. Maier, J. Appl. Phys. **92**, 549 (2002).
[4]M. A. Capano, R. Santhakumar, R. Venugopal, M. R. Melloch, and J. A. Cooper,Jr., J. Electron. Mater. **29**, 210 (2000).
[5]Y. Negoro, K. Katsumoto, T. Kimoto, and H. Matsunami, J. Appl. Phys. **96**, 224 (2004).
[6]F. Schmid and G. Pensl, Appl. Phys. Lett. **84**, 3064 (2004).
[7]M. Ikeda, H. Matsunami, and T. Tanaka, Phys. Rev. B **22**, 2842 (1990).
[8]H. Itoh, T. Troffer, and G. Pensl, Material Science Forum 264–268, 685 (1998).
[9]Y. Negoro, T. Kimoto, H. Matsunami, F. Schmid, and G. Pensl, J. Appl. Phys. **96**, 4916 (2004).
[10]T. Kimoto, O. Takemura, H. Matsunami, T. Nakata, and M. Inoue, J. Electron. Mater. **27**, 358 (1998).
[11]N. S. Saks, A. K. Agarwal, S.-H. Ryu, and J. W. Palmour, J. Appl. Phys. **90**, 2796 (2001).
[12]M. V. Rao, J. A. Gardner, P. H. Chi, O. W. Holland, G. Kelner, J. Kretchmer, and M. Ghezzo, J. Appl. Phys. **81**, 6635 (1997).
[13]T. Troffer, M. Schadt, T. Frank, H. Itoh, G. Pensl, J. Heindl, H. P. Strunk, and M. Maier, Phys. Status Solidi A **162**, 277 (1997).
[14]M. Laube, G. Pensl, and H. Itoh, Appl. Phys. Lett. **74**, 2292 (1999).
[15]H. Bracht, N. A. Stolwijk, M. Laube, and G. Pensl, Appl. Phys. Lett. **77**, 3188 (2000).
[16]R. Kumar, J. Kozima, and T. Yamamoto, Jpn. J. Appl. Phys., Part 1 **39**, 2001 (2000).
[17]Y. Negoro, K. Katsumoto, T. Kimoto, and H. Matsunami, Mater. Sci. Forum **457–460**, 933 (2004).
[18]H. Okushi and Y. Tokumaru, Jpn. J. Appl. Phys., Suppl. **20–1**, 261 (1981).
[19]S. Weiss and R. Kassing, Solid-State Electron. **31**, 1733 (1988).
[20]J. M. Bluet, J. Pernot, J. Camassel, S. Contreras, J. L. Robert, J. F. Michaud, and T. Billon, J. Appl. Phys. **88**, 1971 (2000).
[21]K. A. Jones *et al.*, J. Appl. Phys. **96**, 5613 (2004).
[22]K. Danno, T. Kimoto, and H. Matsunami, Appl. Phys. Lett. **86**, 122104 (2005).
[23]L. Storasta, F. H. C. Carlsson, S. G. Sridhara, J. P. Bergman, A. Henry, T. Egilsson, A. Hallén, and E. Janzén, Appl. Phys. Lett. **78**, 46 (2001).
[24]A. Schöner, N. Miyamoto, T. Kimoto, and H. Matsunami, Mater. Sci. Forum **353–356**, 451 (2001).
[25]T. Troffer, Ch. Häßler, G. Pensl, K. Hölzlein, H. Mitlehner, and J. Völkl, Inst. Phys. Conf. Ser. **142**, 281 (1996).
[26]S. G. Sridhara, L. L. Clemen, R. P. Devaty, W. J. Choyke, D. J. Larkin, H. S. Kong, T. Troffer, and G. Pensl, J. Appl. Phys. **83**, 7909 (1998).
[27]T. Frank, T. Troffer, G. Pensl, N. Nordell, S. Karlsson, and A. Schöner, Mater. Sci. Forum **264–268**, 681 (1998).
[28]A. Gali, T. Hornos, P. Deák, N. T. Son, E. Janzén, and W. J. Choyke, Mater. Sci. Forum **483–485**, 519 (2005).